
Technical report, IDE1023 , November 30, 2010

SVI Estimation of the Implied Volatility by Kalman Filter

Master's Thesis in Financial Mathematics

Burnos Sergey and ChaSing Ngow



School of Information Science, Computer and Electrical Engineering
Halmstad University

SVI Estimation of the Implied Volatility by Kalman Filter

Burnos Sergey and Chasing Ngow

Halmstad University
Project Report IDE1023

Master's thesis in Financial Mathematics, 15 ECTS credits

Supervisor: Assoc.Prof. Mikhail Nечаев
Examiner: Prof. Ljudmila A. Bordag
External referees: Prof. Mikhail Babich

November 30, 2010

Department of Mathematics, Physics and Electrical Engineering
School of Information Science, Computer and Electrical Engineering
Halmstad University

Preface

The work on this paper has been very enriching as well as exciting. We would like to acknowledge the following people who have guided us throughout this project. First of all, our deepest appreciation to professor Mikhail Nечаев, our thesis supervisor for giving us this wonderful opportunity to work on this thesis and his guidance throughout the research area. We would also like to thank professor Ljudmila Bordag, our course coordinator and professor Mikhail Babich for their valuable teaching and guidance. Lastly, we would like to thank all our peers working with us and those who has giving us their support throughout this research. This thesis will not be made possible without your support. Thank you.

Abstract

To understand and model the dynamics of the implied volatility smile is essential for trading, pricing and risk management portfolio. We suggest a linear Kalman filter for updating of the Stochastic Volatility Inspired (SVI) model of the volatility. From a risk management perspective we generate the 1-day ahead forecast of profit and loss (P&L) of option portfolios. We compare the estimation of the implied volatility using the SVI model with the cubic polynomial model. We find that the SVI Kalman filter has outperformed the others.

Contents

1	Introduction	1
1.1	Motivation	1
1.2	Objectives	2
1.3	Chapters Review	2
2	Literature Review	3
2.1	Volatility	3
2.1.1	Types of the volatility	3
2.2	Dupire's model	4
2.3	The Dynamic of the Implied Volatility (IV)	6
2.4	Features of the Implied volatility	7
3	S&P Data Set and Option Portfolios	11
3.1	Properties of S&P 500	11
3.1.1	Liquidity	12
3.1.2	Moneyness	12
3.2	The Option Portfolios	13
3.2.1	Short straddle	13
3.2.2	Long risk reversal	14
3.2.3	Long butterfly spread	15
4	Stochastic Volatility Inspired model	17
4.1	The SVI model	17
4.2	Parameters of the SVI	18
4.2.1	Slopes and minimum	18
4.2.2	Arbitrage constraints	18
4.2.3	Limiting cases $s \rightarrow 0$ and $s \rightarrow \infty$ (almost-affine smiles)	19
4.3	Dimension reduction	20
4.4	The calibration of the SVI model.	21
4.4.1	The calibration procedures of the parameter c	21
4.4.2	The calibration of the parameter s	22

5 Procedures of a Kalman Filtering Estimation	25
5.1 The Kalman Filter	25
5.2 The cubic polynomial interpolation model	28
5.3 The SVI model	29
5.4 The Kalman filter estimation	29
6 Application of the Kalman filter to an option portfolio P&L forecasting	31
6.1 The P-C-Parity	31
6.2 The Portfolio 1: a Short Straddle	31
6.3 The Portfolio 2: a Risk Reversal portfolio	32
6.4 Testing procedures of option portfolios	33
7 Results	35
7.1 The Implied Volatility Result Analysis	35
7.2 The Portfolios Result Analysis	37
7.2.1 The Portfolio of a Short Straddle (V^{SS})	37
7.2.2 The Portfolio of the Long Risk Reversal (V^{RR})	38
8 Conclusions	41
Bibliography	43
Appendix	47
8.1 The Least Square Method	47

Chapter 1

Introduction

1.1 Motivation

With the introducing of the Black-Scholes model to the financial market by Fischer Black and Myron Scholes in 1973, the financial market has entered a new era. It is assumed that the underlying asset is traded in a frictionless market, which has a constant volatility. With the absence of arbitrage, the Black-Scholes formula calculates the prices of the options based on the underlying asset. This useful and yet powerful the Black-Scholes option-pricing model is widely used in a practice since it was being introduced. It was generally being accepted due to ease of calculation and robustness.

It is commonly used to calculate the option prices given the volatility σ and parameters (S_t, K, r, T) . The Black-Scholes implied volatility is a unique volatility parameter derived from the Black-Scholes formula using market option prices. In general, the volatility of option prices is actually non-constant. It varies with respect to strike levels and different maturities. An understanding of the characteristics of the volatility helps us to construct an implied volatility skew (fixed maturity), the term structure of the volatility (fixed strike) or an implied volatility surface. In details we explain these connections in the Chapter 2.3.

The implied volatility described in the Black-Scholes model is the most difficult parameter to understand and it has an important role in the financial world. With the increase usage and complexity of the derivatives raises a need for a framework for better understanding of the dynamics of the volatility. Hence, it can provide us with an accurate and consistent pricing. The implied volatility can be further implemented for the hedging of portfolio's risk and trading of a wide range of derivative products.

1.2 Objectives

The main objectives of the research in our master project is to

1. Understand and develop the Kalman Filtering procedures for an estimation of the dynamics of the Implied Volatility smile.
2. Generate the 1-day ahead forecast of the implied volatility using the Kalman Filter model against moneyness.
3. Calculate the Profit and Losses of the option's portfolios.

It is essential to have a reliable forecast for the evolution of the Implied Volatility curve:

- Up-to-date indication of the market option prices to support trading and hedging.
- To provide an efficient and dynamical risk management of the option's portfolios.

The main objective of the research study is to develop the Kalman Filtering procedures to forecast the dynamics of the implied volatility smile. In addition, to implement an application for the Kalman Filtering model: to estimate the Profits and Losses (P&L) of the option's portfolios. This approach can be further research and refine to implement on VaR-based or CRM-based risk estimation with the use of the Kalman filter extrapolation technique.

1.3 Chapters Review

Chapter 1 presents the reader a general idea to use an implied volatility in the financial market. In chapter 2 we discuss various types and features of a volatility. Chapter 3 introduces the properties of data set and type of option portfolios. Chapter 4 discusses the Stochastic Volatility Inspired model. Chapter 5 describes the Kalman Filter model and the procedures of the Kalman Filtering estimation. Chapter 6 discusses the application of the Kalman Filter forecasting technique for option portfolios. In chapter 7 we analyze the results. Finally, we summarized the study with a short conclusion of our thesis and possible future research directions.

Chapter 2

Literature Review

2.1 Volatility

A volatility is often described as a fluctuation of the return of the underlying asset which used in the option pricing before the option maturity. It is also used to quantify the risk of the financial instrument over a specific period of time.

Generally, the volatility is expressed in a annualized term. The annualized volatility σ is the standard deviation of the financial instruments logarithmic returns over a year. The generalized volatility σ_T over a period of time horizon T in years is equal to: $\sigma_T = \sigma\sqrt{T}$.

As the volatility is a statistical measure of a distribution of the return of the underlying asset, the high volatility term refers to a potential of the underlying asset value to spread over a large range of price movement over a period of time, and the prices of the underlying can move drastically over a short period of time in either direction. On the other hand, low volatility term refers to the stability of the underlying asset value within a small range of price movement over a given period of time.

2.1.1 Types of the volatility

The volatility of the option pricing can be further categorized as follows:

- Historical/realized,
- Actual/local,
- Implied,
- Futures.

A historical or realized volatility is a measurement of randomness of the return of the underlying asset over a specific period of time in the past. This is a backward-looking estimation of the future volatility.

An actual or local volatility (σ_t) is a measurement of randomness of the return of the underlying asset at a specific time. It is expressed as a function of the current asset S_t and the time t .

An implied volatility refers to the volatility that can be input into the Black-Scholes option pricing formula to obtain the market option price. It is often described as the market's view of the future actual volatility before maturity. It is expressed as a function of the strike K and maturity T . (refer to section 2.3)

A future volatility refers to a forecast of the volatility of the return of the underlying asset over a time period in the future.

2.2 Dupire's model

An underlying asset value of the non-dividend paying index/stock/ has the non-negative price S_t . The underlying asset value is modeled as a random walk in accordance to the equation

$$dS/S = \mu_t dt + \sigma(S_t, t) dZ, \quad (2.1)$$

where μ_t is a drift, $\sigma(S_t, t)$ is the local volatility and dZ is the Wiener process.

A collection of the European option prices $C(S_0, K, T)$ for the current stock price, different strikes K and maturity times T is expressed as

$$C(S_0, K, T) = \int_K^\infty dS_T \varphi(S_T, T; S_0)(S_T - K), \quad (2.2)$$

where $\varphi(S_T, T; S_0)$ is the pseudo-probability density of the final spot at time T .

Under risk neutrality condition with application of Ito's lemma, we obtained the partial differential equation for the function of the stock price which is the generalization of the Black-Scholes formula

$$\frac{\partial C}{\partial T} = -\frac{1}{2}\sigma^2 K^2 \frac{\partial^2 C}{\partial K^2} + r_t \left(C - K \frac{\partial C}{\partial K} \right), \quad (2.3)$$

where r_t is the risk free rate.

The pseudo-probability risk neutral density function $\varphi(K, T; S_0) = \frac{\partial^2 C}{\partial K^2}$ must satisfy the Fokker -Planck equation. Under the Fokker-Planck equation, it evolves to

$$\frac{1}{2} \frac{\partial^2}{\partial S_T^2} (\sigma^2 S_T^2 \varphi) - S \frac{\partial}{\partial S_T} (\mu S_T \varphi) = \frac{\partial \varphi}{\partial T}. \quad (2.4)$$

Differentiating (2.2) with respect to K gives us

$$\begin{aligned} \frac{\partial C}{\partial K} &= - \int_K^\infty dS_T \varphi(S_T, T; S_0), \\ \frac{\partial^2 C}{\partial K^2} &= \varphi(K, T; S_0). \end{aligned} \quad (2.5)$$

Now, differentiating (2.2) with respect to time results in

$$\begin{aligned} \frac{\partial C}{\partial T} &= \int_K^\infty dS_T \left\{ \frac{\partial}{\partial T} \varphi(S_T, T; S_0) \right\} (S_T - K) \\ &= \int_K^\infty dS_T \left\{ \frac{1}{2} \frac{\partial^2}{\partial S_T^2} (\sigma^2 S_T^2 \varphi) - \frac{\partial}{\partial S_T} (\mu S_T \varphi) \right\} (S_T - K). \end{aligned} \quad (2.6)$$

Finally, integrating by parts gives:

$$\begin{aligned} \frac{\partial C}{\partial T} &= \frac{\sigma^2 K^2}{2} \varphi + \int_K^\infty dS_T \mu S_T \varphi \\ &= \frac{\sigma^2 K^2}{2} \frac{\partial^2 C}{\partial K^2} + \mu(T) \left(-K \frac{\partial C}{\partial K} \right), \end{aligned} \quad (2.7)$$

which is the Dupire equation when the underlying asset has a drift μ . If we express the option price as a function of the forward price, $F_T = S_0 \exp \left\{ \int_0^T \mu(t) dt \right\}$, we obtain the same expression minus the drift term.

$$\frac{\partial C}{\partial T} = \frac{1}{2} \sigma^2 K^2 \frac{\partial^2 C}{\partial K^2}, \quad (2.8)$$

where C now represents $C(F_T, K, T)$.

By inverting the formula (2.8), we obtained the local volatility

$$\sigma^2(K, T, S_0) = \frac{\frac{\partial C}{\partial T}}{\frac{1}{2} K^2 \frac{\partial^2 C}{\partial K^2}}. \quad (2.9)$$

Equation (2.9) is a definition of the local volatility function under the Dupire's model. Therefore given a complete set of the European option prices of all strikes and maturity, we can obtain the local volatility structure.

2.3 The Dynamic of the Implied Volatility (IV)

The market prices of the options are modeled as a function of the Black-Scholes implied volatility under the Black-Scholes option pricing model. Implied volatility in the BS model depends strongly on the strike K and the maturity T of the European option. Given the arbitrage free $C(K; T)$, the market price of the European call value with strike price $K > 0$ and maturity T at time $t \in [0; T]$. The BS implied volatility $\sigma(K; T)$ is defined as the value of the volatility parameter which is a solution of the equation, where the option price given by the Black-Scholes model is equal to

$$C(K, T) = C_{BS}(S_t, t; K, r, T, \sigma(K, T)) = S_t N(d_1) - K e^{-r(T-t)} N(d_2),$$

where

$$\begin{aligned} d_1 &= \frac{\log S/K + (r + \frac{1}{2}\sigma^2)(T - t)}{\sigma\sqrt{T - t}}, \\ d_2 &= \frac{\log S/K + (r - \frac{1}{2}\sigma^2)(T - t)}{\sigma\sqrt{T - t}}. \end{aligned}$$

As the implied volatility is time dependent, we use

$$\sqrt{\frac{1}{T-t} \int_t^T \sigma(\tau)^2 d\tau},$$

and replace $\sigma\sqrt{T - t}$ in the formula for d_1 and d_2

$$\begin{aligned} d_1 &= \frac{\log S/K + r(T - t) + \frac{1}{2} \int_t^T \sigma(\tau)^2 d\tau}{\sqrt{\int_t^T \sigma(\tau)^2 d\tau}}, \\ d_2 &= \frac{\log S/K + r(T - t) - \frac{1}{2} \int_t^T \sigma(\tau)^2 d\tau}{\sqrt{\int_t^T \sigma(\tau)^2 d\tau}}. \end{aligned}$$

Since we know the local volatility $\sigma(t)$, we can find the value of the options. We are able to obtain the implied volatility from the local volatility:

$$\sigma(t) \Rightarrow \sigma_{IV}(t^*, T).$$

Where $\sigma(t^*, T)$ refers to the implied volatility measured at the time t^* of a European option with the maturity time T .

As we can observe the $\sigma_{IV}(t^*, T)$ backward-looking estimation for deducing of the function of the local volatility $\sigma(t)$ is consistent with the implied volatility,

$$\sigma_{IV}(t^*, T) \Rightarrow \sigma(t).$$

Due to the time dependence, we need to ensure the consistent option pricing

$$\sqrt{\frac{1}{T-t} \int_t^T \sigma(\tau)^2 d\tau} = \text{implied volatilities.}$$

2.4 Features of the Implied volatility

This section describes the behavior pattern of the implied volatility as a function of strike levels and maturities of the option prices.

The Volatility Smile

The volatility smile describes the relationship between the implied volatility and strike prices for fixed maturity option series.

Definition 1 For any fixed maturity time T , $T \leq T^*$, the function $\sigma_t(K, T)$ of the implied volatility against strike price K , $K > 0$, is called the implied volatility smile at time $t \in [0, T]$.

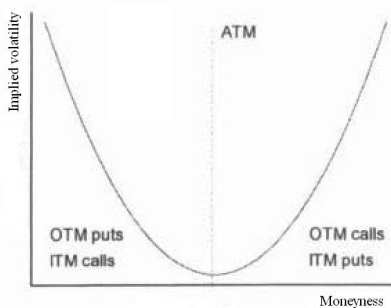


Figure 2.1. The volatility smile.

Volatility smile is an observed pattern which displays that the ATM options have a lower implied volatility than ITM or OTM options. The volatility smile pattern is observed after the 1987 crash. (Derman 1994)

The volatility smile curve indicates the premium charged for OTM puts and ITM calls which are above the Black-Scholes option prices computed with the ATM implied volatility. The shape of the implied volatility is usually a

plot against the log moneyness. This is known as both the volatility smile as well as the volatility skew for the case when it is not symmetrical.

Term Structures of the Volatility

Term structures of the volatility describes the relationship between implied volatility and fixed strike options from correspondent expiration time.

Definition 2 For any fixed strike price K , $K > 0$, the function $\sigma_t(\cdot, T)$ of implied volatility against maturity time T , $T \leq T^*$, is known as term structure of implied volatility or volatility of term structure at time $t \in [0, T]$.

The strike price K is usually chosen to be the ATM strike. Then the shape of the curve is described as normal if the implied volatility for the option with longer maturity dates are higher than those for the option with shorter maturity dates. It is described as an inverse shape if the short-dated option has higher implied volatility compared to the long dated option. Finally, it is described as a flat if the implied volatility is plotted as a horizontal line against the maturity dates.

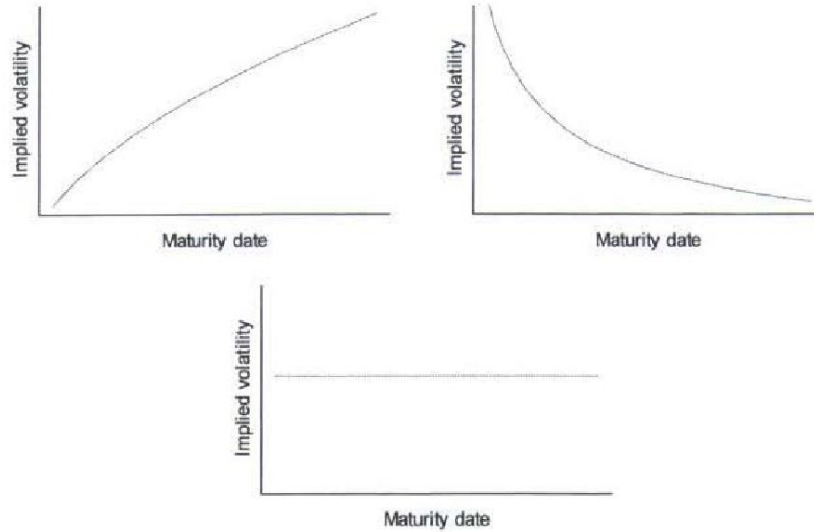


Figure 2.2. The typical forms of the term structure of a volatility.

The Volatility Surfaces

The volatility surface combines the volatility smile with term structure of volatility to construct the implied volatility for market consistency of the options pricing with respect to any strikes levels and maturities.

Definition 3 For any time $t \in (0, T^*)$, the function $\sigma_t : (0, \infty) \times (t, T^*] \rightarrow \mathbb{R}_+$, which assigns each strike price and maturity time tuple (K, T) its implied volatility $\sigma_t(K, T)$ is referred to as the implied volatility surface.

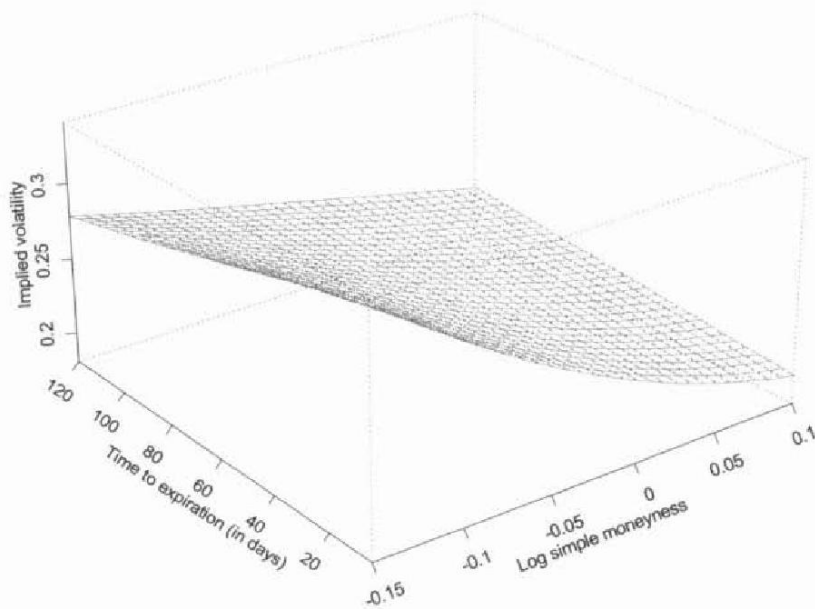


Figure 2.3. The volatility surface.

Chapter 3

S&P Data Set and Option Portfolios

3.1 Properties of S&P 500

The option's underlying, Standard & Poor's 500 (S&P 500) is introduced since 1957 as a capitalization weighted performance index¹. It consists of the prices of 500 large cap common stock actively traded in the United States. The index mainly focuses on U.S.-based companies and a few companies having headquarters in other countries.

Our research database consists of daily closing options prices and futures prices on the S&P500 index, traded in Chicago Mercantile Exchange (CME) over the period from Oct 2009- May 2010. We use the European options with monthly maturity. The futures contract is based on the quarterly futures contract for the nearest 2 months.

The first 5 months of the data are employed to estimate the parameters of the models, while the data of the last months is used to assess the forecasting properties of the Kalman Filter Model.

The rollover of the futures contract prices are done within the two weeks to maturity. While the rollover of the monthly maturity option contracts were done within 3 days to maturity to the following month. This is to ensure liquidity of the contracts with a wide range of strikes.

We apply the usual no-arbitrage limitation for the futures options to filter the option data. We also exclude option data with extreme strikes and data

¹A **capitalization-weighted index** also known as market-value-weighted index. It is an index whose components are weighted according to the total market value of their outstanding shares. The impact of a component's price change is proportional to the issue's overall market value, which is the share price times the number of shares outstanding.

with a low liquidity. After the data filtering, our data set has an average number of strikes/option of 55 a day of the future contract with a minimum of 39 and maximum of 83. The risk-free rate is fixed at 0.25 %.

3.1.1 Liquidity

Liquidity of the contract is important as it ensures the option contract be actively traded in a consistent volume and market depth environment.

The liquidity of the option contract is concentrated on short term option and declines exponentially with increase time to maturity. Liquidity also concentrated on active strike prices which are ATM or OTM but close to the underlying prices. The option trades distribution across degrees of moneyness is skewed to the right. This means OTM option are traded more frequently as compared to ITM option.

3.1.2 Moneyness

It is the relationship between the strike price of an option and the underlying asset price. It is also a description of the intrinsic value of an option at its current state. The intrinsic value of the option is often described as,

1. At the money (ATM), if the option strike price is same as the underlying asset price $S_t = K$.
2. In the money (ITM), if the option has a positive intrinsic value as well as time value.
 - Call option: $S_t > K$,
 - Put option: $K > S_t$.
3. Out of the money (OTM), if the option has no intrinsic value.
 - Call option: $S_t < K$
 - Put option: $K < S_t$

The measure of moneyness m , (Natenberg 1994), is expressed as

$$\frac{\ln(K/F_t)}{\sqrt{\tau}},$$

where underlying is the future price, $F_t = S_t e^{rT}$. The natural log of the ratio between the strike and the underlying future price is normalized by the square root of time to maturity. The normalization helps to correct the effect of τ shrinking over time.

3.2 The Option Portfolios

In order to assess the practical use of the Kalman Filter model for forecasting the dynamics of the volatility curve, we test the model with different option portfolios. From risk management perspectives, we analyze the effectiveness of the prediction with portfolios sensitivity to changes of the different nature in the volatility curve. These are the three option portfolios:

3.2.1 Short straddle

Short call and short put for ATM options with the same strike price and maturity date.

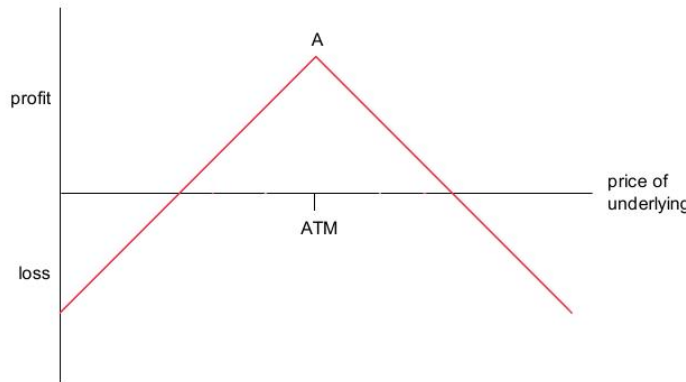


Figure 3.1. The payoff of a short straddle.

Market expectation: market neutral or volatility bearish. P&L: limited profit with unlimited loss potential. Payoff: if the underlying S_t is close to strike price K , the straddle leads to a profit. However, if the underlying S_t has a sufficiently large movement in price level in either direction, it leads to a loss. Therefore this option portfolio anticipates a period of low or decreasing volatility, the underlying is not expected to move drastically.

Payoff table for the short straddle:

	Payoff for call	Payoff for put	Total payoff
$S_T < K$	C	0	C
$S_T > K$	0	P	P

Table 3.1. The payoff structure for a short straddle.

It is sensitive to changes in the level of the ATM implied volatility smile.

The value of the option portfolio will decrease (increase) with the increase (decrease) in Implied Volatility level.

3.2.2 Long risk reversal

One short put and one long call for OTM options with the same maturity date (synthetic long underlying). Positive Risk Reversal refers to buying a call option more expensive than a put due to higher implied volatility of a call option. (Bullish sentiment). Negative Risk Reversal refers to selling a put option more expensive than a call due to higher implied volatility of put option. (Bearish sentiment).

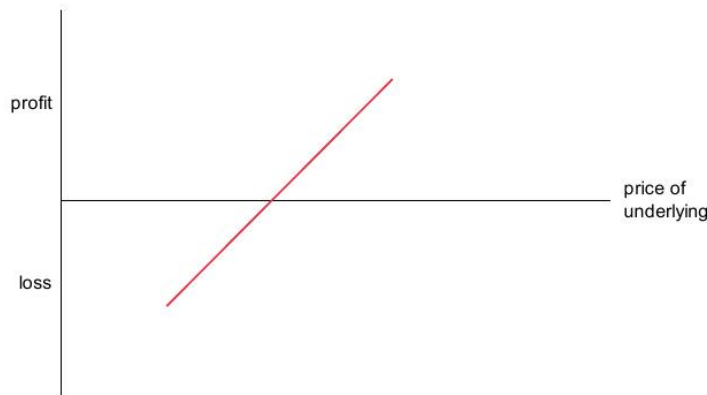


Figure 3.2. The payoff of the long risk reversal

Market expectation: market bullish or volatility neutral. P&L: unlimited profit and unlimited loss potential Payoff: if the underlying S_t trade above the strike price K , the risk reversal leads to a profit. However, if the underlying S_t stay at or below the strike price K , it leads to a loss. Therefore option portfolio anticipates a period of neutral volatility, the underlying is expected to rise.

Payoff Table for the long risk reversal:

	Short OTM put	Long OTM call	Total payoff
$S_T > K$	P	$S_T - K$	$S_T - K + P$

Table 3.2. The payoff data for a long risk reversal.

It is sensitive to the changes in the slope of the Implied Volatility smile. The value of the option portfolio will decrease (increase) with the increase (decrease) steepness of slope of the Implied Volatility smile.

3.2.3 Long butterfly spread

One short call and one short put for ATM options and one long call and one long put for OTM options with same maturity date.

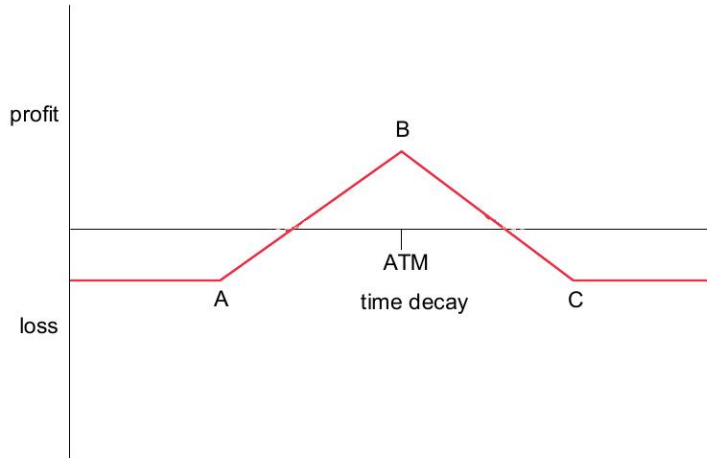


Figure 3.3. The payoff of the long butterfly spread.

Market expectation: direction neutral or volatility bearish. Expect underlying stay near ATM level. It is less risky than shorting straddles or strangles due to it's limited downside exposure. P&L: limited profit and loss potential (due to the net cost of the position for either a rise or a fall in the underlying price.) Payoff: if the underlying S_t is close to the strike price K , the straddle leads to a limited profit. However, if the underlying S_t has a sufficiently large movement in the price level in either direction, it leads to a limited loss. Therefore the option portfolio anticipates a period of low or decreasing volatility, the underlying is not expected to move drastically.

Payoff table for the long butterfly:

	Long OTM call	OTM put	Short ATM call	ATM put	Total payoff
$S_T < K$	0	$K - S_T$	C	0	$K - S_T + C$
$S_T > K$	$S_T - K$	0	0	P	$S_T - K + P$

Table 3.3. The payoff features for a long butterfly spread.

It is sensitive to the changes in the curvature of the Implied Volatility smile. The value of the portfolio will decrease with the decrease in the curvature of the Implied Volatility smile.

Chapter 4

Stochastic Volatility Inspired model

4.1 The SVI model

Jim Gatheral's SVI model [4] is described as follow

$$\sigma_{SVI} = a + b \left(\rho(x - c) + \sqrt{(x - c)^2 + s^2} \right). \quad (4.1)$$

Where the SVI parameters mean

- a estimates the overall ATM level of the implied volatility,
- b captures the the angle between the left and right asymptotes (slopes),
- s determines the smoothness of the vertex,
- ρ determines the orientation of the plot,
- c changes the translation of the plot.

SVI is used to extrapolate the smile point and provide smooth smile. Hence, it facilitates the calibration of the stochastic volatility model for the underlying asset by reconstructing the local volatility smiles via Dupire's formula which interpolate in time.

SVI provides an outstanding calibration performance to single maturity time T . However it has drawback on the least lquare calibration, it is badly affected by the presence of several local minima.

On simple observations on the symmetries of the functional equation (4.1), we can introduce dimension reduction to eliminate the drawback. The

number of parameters are reduced from 5 to 2 (mainly c and s), while the optimization over the remaining 3 parameters is performed explicitly. This method allows us to construct an optimal parameter set which is consistent with the arbitrage free constraint on the slopes of the implied volatility.

4.2 Parameters of the SVI

The parameters a, b, ρ, c and s in general depend on time to maturity τ . Let us assume that the parameters b, s, ρ satisfied the following conditions

$$b > 0, \quad s > 0, \quad \rho \in [-1, 1].$$

4.2.1 Slopes and minimum

Properties of the SVI parametric form are described as the left and the right asymptotes as follow

$$\begin{aligned} \nu_L(x) &= a - b(1 - \rho)(x - c), \\ \nu_R(x) &= a + b(1 + \rho)(x - c). \end{aligned} \tag{4.2}$$

Parameter a in (4.1) is positive and convex w.r.t. x , it has a minimum point with the following properties

- if $\rho^2 \neq 1$, the minimum is $a + bs\sqrt{1 - \rho^2}$ attained at $x^* = c - \frac{\rho s}{\sqrt{1 - \rho^2}}$;
- if $\rho^2 = 1$, σ_{SVI} is non-increasing for $\rho = -1$ and non-decreasing for $\rho = 1$ and
 - if $s \neq 0$, σ_{SVI} is strictly monotone and the minimum is never attained (nevertheless, $\sigma_{SVI} \rightarrow a$ for very positive or negative x);
 - if $s = 0$, σ_{SVI} has the shape of a Put or Call payoff of strike c (σ_{SVI} is worth a for $x \geq c$ if $\rho = -1$ and for $x \leq c$ if $\rho = 1$).

4.2.2 Arbitrage constraints

A necessary condition is required for the absence of arbitrage as a constraint on the maximal slope of the implied volatility

$$b \leq \frac{4}{(1 + |\rho|)T}. \tag{4.3}$$

4.2.3 Limiting cases $s \rightarrow 0$ and $s \rightarrow \infty$ (almost-affine smiles)

As considered in the case $\rho^2 = 1$, letting $s \rightarrow 0$ gives a piecewise affine parameterization of the volatility. The following two regions, where $x < c$ and $x > c$, the volatility is represented as

$$\sigma_{SVI} = a + b(\rho \mp 1)(x - c). \quad (4.4)$$

Implied volatility smiles are well-fitted with an affine parametrization $\sigma_{SVI} = px + q$. If we let $s \rightarrow 0$ and take c to be greater than the largest observed log-moneyness, then matching of the two relevant quantities, i.e. smile slope p and intercept q , yields the two equations

$$\begin{aligned} b(\rho - 1) &= p, \\ a - bc(\rho - 1) &= q, \end{aligned}$$

correspondent to infinitely many choices of parameters of a, b, ρ , which leads to many solutions.

If we limit $s \rightarrow \infty$ and $a \rightarrow \infty$, we can allow a to be non-negative value

It follows from that the positivity of the parameterisation of the equation (4.2) can be achieved by attaining the minimum σ_{SVI} to be non-negative

$$a \geq -bs\sqrt{1 - \rho^2}.$$

If the minimum is not attained, then $\rho^2 = 1$ and the condition becomes $a \leq 0$. Assume $a > 0$ and $s \gg 1$, we obtain

$$\begin{aligned} \sigma_{SVI} &= a + b \left(\rho(x - c) + \sqrt{s + (x - c)^2} \right) = \\ &= -|a| + b\rho(x - c) + b\rho\sqrt{1 + \frac{(x - c)^2}{s^2}} \sim \\ &\sim -|a| + b\rho(x - c) + b\rho \left(1 + \frac{(x - c)^2}{2s^2} \right) \sim \\ &\sim_{|a|=b\rho} b\rho(x - c) + b\frac{(x - c)^2}{2s}. \end{aligned}$$

Hence

$$\lim_{s \rightarrow \infty, a \rightarrow -\infty, |a|=bs} \sigma_{SVI} = b\rho(x - c)$$

for any value of x , and this corresponds again to an affine smile whose slope and intercept identify the product $b\rho$ and the parameter c , but not b, ρ and c separately.

The main objective of the calibration is to acquire the stability conditions. In order to avoid the instability behavior condition, we limit the calibration of the SVI model parameters by the following boundaries:

$$\begin{aligned} s &\geq s_{min} > 0, \\ a &\geq 0. \end{aligned} \tag{4.5}$$

The positive lower bound s_{min} for s is set at the value of 0.004.

At the same time, we limit a to be non-negative value. It was done to avoid the instability behavior when $s \rightarrow \infty$ and $a \rightarrow \infty$. Finally, we would like to limit an upper bound for s , however this would not prevent the situation of coupling of low values of a and high values of s , where s tends to s_{max} and a leads to negative value. Therefore, we limit the upper bound on a to be

$$a \leq \max_i \{\sigma_{SVI_i}\}. \tag{4.6}$$

4.3 Dimension reduction

The SVI model suffers from the least square calibration which lead to an optimization problem in dimension 5. This problem can be eliminated by simple observation on the properties of the functional form (4.1), and reformulate the equation from dimension 5 to 2. By the means of change of variables

$$y = \frac{x - c}{s},$$

the SVI parametrization can be transformed into

$$\tilde{\sigma}_{SVI} = aT + bsT \left(\rho y + \sqrt{y^2 + 1} \right).$$

For fixed values of c and s , the implied volatility curve is supported by a , ρ and the product of bs . Thus we can redefine the parameters as

$$\begin{aligned} e &= bsT, \\ d &= \rho bsT, \\ \tilde{a} &= aT, \end{aligned}$$

where σ_{SVI} is linearly depend on parameters \tilde{a} , d and e .

$$\tilde{\sigma}_{SVI}(y) = \tilde{a} + dy + e\sqrt{y^2 + 1}. \tag{4.7}$$

Therefore, given the fixed value for c and s , we are looking for the solution of the problem

$$(P_{c,s}) \quad \min_{(e,d,\tilde{a}) \in D} f_{\{y_i, \sigma_{SVI_i}\}}(e, d, \tilde{a}),$$

where $f_{\{y_i, \sigma_{SVI_i}\}}$ is the cost function

$$f_{\{y_i, \sigma_{SVI_i}\}}(e, d, \tilde{a}) = f(e, d, \tilde{a}) = \sum_{i=1}^n \left(\tilde{a} + dy_i + e\sqrt{y_i^2 + 1} - \tilde{\sigma}_{SVI_i} \right)^2,$$

with $\tilde{\sigma}_{SVI_i} = T\sigma_{SVI_i}$, and D is the compact and convex domain (a parallelepiped)

$$D = \begin{cases} 0 \leq e \leq 4s, \\ |d| \leq e \text{ and } |d| \leq 4s - e, \\ 0 \leq \tilde{a} \leq \max_i \tilde{\sigma}_{SVI_i}. \end{cases} \quad (4.8)$$

which is obtained from the bounds (4.3) and (4.5)-(4.6) on the parameters b , ρ and a . We let (e^*, d^*, \tilde{a}^*) denote the solution of $P_{c,s}$ and (a^*, b^*, ρ^*) be the corresponding triplet for a , b , ρ . Finally the complete calibration problem is

$$(P) \quad \min_{c,s} \sum_{i=1}^n \left(\sigma_{SVI_{c,s,a^*,b^*,\rho^*}}(x_i) - \sigma_{SVI_i} \right)^2.$$

4.4 The calibration of the SVI model.

The purpose of the calibration is to make sure that the output of the model matches the data in the financial market. As the movement of the financial asset does not behave as clearly as the way we define the law of physics, it is mainly driven by human behavior and sentiment. Therefore, we need to calibrate the system model by setting conditions to ensure that the obtained output data is closely relevant to the financial market.

As mentioned in the previous section, we can reduce the complexity of the SVI model by reducing the dimension from 5 to 2. From the observation, we can fix the c and s parameters in the SVI equation.

4.4.1 The calibration procedures of the parameter c

The parameter c describes the translation of the implied volatility curve along log forward moneyness on x -axis. The plot (4.1) has four solid lines. The black solid line is the implied volatility curve obtained from Black-Scholes formula. The green solid line refers to the SVI implied volatility

curve with no translation, $c = 0$. The blue and red solid lines refer to the SVI implied volatility with translation of $c = 0.05$ and $c = -0.05$ respectively. The purpose of calibration is to fit the estimated SVI implied volatility curve as close as possible to the Black-Scholes implied volatility curve. From the blue line we have assumed the log forward moneyness is greater than zero which indicates that the forward value of the underlying asset has risen above the initial value. From the plot we observe the curve which is translated to the right. On the other hand, the red line shows that the log forward moneyness is less than zero which indicates that the forward value of the underlying asset has fallen below the initial value. This can be observed with the translation of the red line to the left.

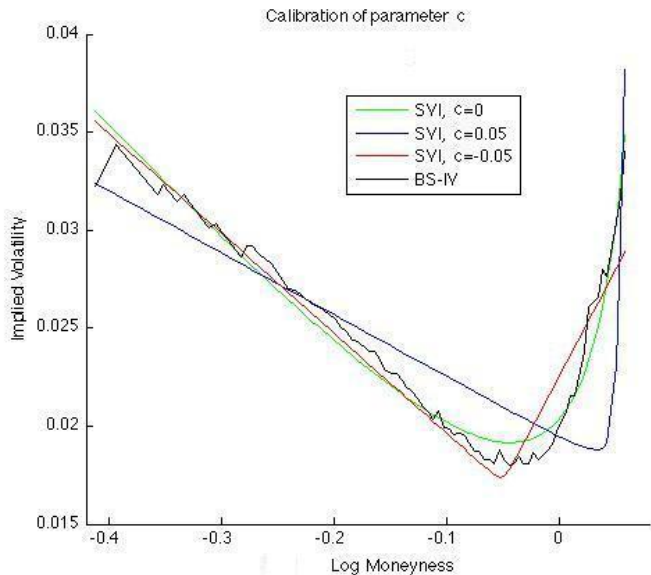


Figure 4.1. The market implied volatility and the SVI implied volatility with translation $c = 0, c = 0.05$ and $c = -0.05$.

4.4.2 The calibration of the parameter s

The parameter s describes the smoothness of the curvature of the implied volatility curve and the plot (4.2) includes four solid lines. The black solid line is the implied volatility curve obtained from the Black-Scholes formula. The green solid line refers to the SVI implied volatility curve with best fit, $s = 0.004$. The blue, red and magenta solid lines display the SVI implied volatility with change of curvature of $s = 0.01, 0.1$ and 1 respectively. Generally, for the short term contract, we select a value of s ranging from 0.004 to

0.01. These curves displayed a steeper and sharper curvature of the implied volatility. While for the longer term contract, we can choose to increase the value of s to achieve a smooth implied volatility curve that fits closer to the Black-Scholes implied volatility curve. The curve has a more curvature.

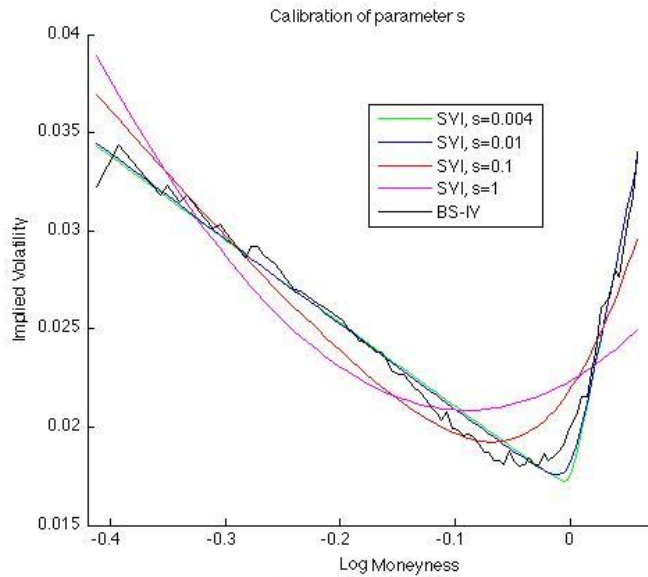


Figure 4.2. The market implied volatility and the SVI implied volatility with the smoothness $s = 0.04, s = 0.01, s = 0.1$ and $s = 1$.

Chapter 5

Procedures of a Kalman Filtering Estimation

5.1 The Kalman Filter

According to [2], let us assume that $(x, \sigma_{IV}) = ((x_t), (\sigma_{IVt}))$ is a partially observed sequence, where

$$x_t = (x_1(t), \dots, x_k(t)), \quad \sigma_{IVt} = (\sigma_{IV1}(t), \dots, \sigma_{IVl}(t)).$$

The recurrent equations, which govern our sequence (x, σ_{IV}) , are

$$\begin{aligned} x_{t+1} &= a_0(t, \sigma_{IV}) + a_1(t, \sigma_{IV})x_n + b_1(t, \sigma_{IV})\varepsilon_1(t+1) + b_2(t, \sigma_{IV})\varepsilon_2(t+1), \\ \sigma_{IVt+1} &= A_0(t, \sigma_{IV}) + A_1(t, \sigma_{IV})x_n + B_1(t, \sigma_{IV})\varepsilon_1(t+1) + B_2(t, \sigma_{IV})\varepsilon_2(t+1). \end{aligned} \quad (5.1)$$

Where

$$\varepsilon_1(t) = (\varepsilon_{11}(t), \dots, \varepsilon_{1k}(t)) \quad \text{and} \quad \varepsilon_2(t) = (\varepsilon_{21}(t), \dots, \varepsilon_{2l}(t))$$

are independent Gaussian vectors with independent components, which are normally distributed with parameters 0 and 1.

The functions

$$a_0(t, \sigma_{IV}) = (a_{01}(t, \sigma_{IV}), \dots, a_{0k}(t, \sigma_{IV})) \quad \text{and} \quad A_0(t, \sigma_{IV}) = (A_{01}(t, \sigma_{IV}), \dots, A_{0l}(t, \sigma_{IV}))$$

are vector functions, which depend for a given t only on $\sigma_{IV0}, \dots, \sigma_{IVt}$.

The matrix functions

$$a_1(t, \sigma_{IV}) = \left\| a_{ij}^{(1)}(t, \sigma_{IV}) \right\|, \quad b_1(t, \sigma_{IV}) = \left\| b_{ij}^{(1)}(t, \sigma_{IV}) \right\|, \quad b_2(t, \sigma_{IV}) = \left\| b_{ij}^{(2)}(t, \sigma_{IV}) \right\|,$$

$$A_1(t, \sigma_{IV}) = \left\| A_{ij}^{(1)}(t, \sigma_{IV}) \right\|, \quad B_1(t, \sigma_{IV}) = \left\| B_{ij}^{(1)}(t, \sigma_{IV}) \right\|, \quad B_2(t, \sigma_{IV}) = \left\| B_{ij}^{(2)}(t, \sigma_{IV}) \right\|$$

depend on σ_{IV} without looking ahead and have orders $k \times k, k \times k, k \times l, l \times k, l \times k, l \times l$, respectively. We assume that the initial vector (x_0, σ_{IV0}) is independent of the sequences $\varepsilon_1 = (\varepsilon_1(t))$ and $\varepsilon_2 = (\varepsilon_2(t))$.

For the existing solution of the system (5.1) with finite second moments, we suppose that

$$\mathbb{E}(\|x_0\|^2 + \|\sigma_{IV0}\|^2) < \infty, \quad \left| a_{ij}^{(1)}(t, \sigma_{IV}) \right| \leq C, \quad \left| A_{ij}^{(1)}(t, \sigma_{IV}) \right| \leq C,$$

and if $f(t, \sigma_{IV})$ is any of the functions $a_{0i}, A_{0j}, b_{ij}^{(1)}, b_{ij}^{(2)}, B_{ij}^{(1)}$ or $B_{ij}^{(2)}$ then $\mathbb{E}|f(t, \sigma_{IV})|^2 < \infty$ for any $t = 0, 1, \dots$. According to these assumptions, (x, σ_{IV}) has $\mathbb{E}(\|x_t\|^2 + \|\sigma_{IVt}\|^2) < \infty$, for any $t \leq 0$.

$\mathcal{F}_t^{\sigma_{IV}} = \sigma\{\omega : \sigma_{IV0}, \dots, \sigma_{IVt}\}$ represents the smallest σ -algebra generated by $\sigma_{IV0}, \dots, \sigma_{IVt}$ and

$$m_t = \mathbb{E}(x_t | \mathcal{F}_t^{\sigma_{IV}}), \quad \gamma_t = \mathbb{E}[(x_t - m_t)(x_t - m_t)^* | \mathcal{F}_t^{\sigma_{IV}}].$$

As determined by Theorem 1, §8, Chapter 2, page 237, [2], $m_t = (m_1(t), \dots, m_k(t))$ is an optimal estimator for the vector $x_t = (x_1(t), \dots, x_k(t))$, and

$\mathbb{E}\gamma_t = \mathbb{E}[(x_t - m_t)(x_t - m_t)^*]$ is the matrix of errors of observation. The main problem is to determine these matrices for arbitrary sequences (x, σ_{IV}) governed by equations (5.1). We assume an additional condition on (x_0, σ_{IV0}) , which indicates the conditional distribution $\mathbb{P}(x_0 \leq a | \sigma_{IV0})$ is Gaussian,

$$\mathbb{P}(x_0 \leq a | \sigma_{IV0}) = \frac{1}{\sqrt{2\pi\gamma_0}} \int_{-\infty}^a \exp\left\{-\frac{(x - m_0)^2}{2\gamma_0^2}\right\} dx, \quad (5.2)$$

with parameters $m_0 = m_0(\sigma_{IV0}), \gamma_0 = \gamma_0(\sigma_{IV0})$.

Lemma 1 According to the above assumptions made about the coefficients of (5.1), together with (5.2), the sequence (x, σ_{IV}) is conditionally Gaussian, i. e. the conditional distribution function

$$\mathbb{P}\{x_0 \leq a_0, \dots, x_t \leq a_t | \mathcal{F}_t^{\sigma_{IV}}\}$$

is (\mathbb{P} -a.s.) the distribution function of an t -dimensional Gaussian vector whose mean and covariance matrix depend on $(\sigma_{IV0}, \dots, \sigma_{IVt})$.

See the proof in [2], page 466.

Theorem 1 Assume that (x, σ_{IV}) is a partial observation of the sequence which satisfies the system (5.1) and condition (5.2). Then (m_t, γ_t) comply the following recursion equations:

$$m_{t+1} = [a_0 + a_1 m_t] + [b \circ B + a_1 \gamma_t A_1^*] [B \circ B + A_1 \gamma_t A_1^*]^{\oplus} [\sigma_{IVt+1} - A_0 - A_1 m_t], \quad (5.3)$$

$$\gamma_{t+1} = [a_1 \gamma_t A_1^* + b \circ b] - [b \circ B + a_1 \gamma_t A_1^*] [B \circ B + A_1 \gamma_t A_1^*]^{\oplus} [b \circ B + a_1 \gamma_t A_1^*]^*. \quad (5.4)$$

Here $b \circ b = b_1 b_1^* + b_2 b_2^*$, $b \circ B = b_1 B_1^* + b_2 B_2^*$, $B \circ B = B_1 B_1^* + B_2 B_2^*$.

See the proof in [2], page 467.

Corollary 1 In the case, if the coefficients $a_0(t, \sigma_{IV}), \dots, B_2(t, \sigma_{IV})$ from the system (5.1) do not depend on σ_{IV} we obtain the Kalman-Bucy model, and equations (5.3) and (5.4) for m_t and γ_t describe the Kalman-Bucy filter. We notice that then the conditional and unconditional error matrices y_n are equal, i. e.

$$\gamma_t \equiv \mathbb{E}\gamma_t = \mathbb{E}[(x_t - m_t)(x_t - m_t)^*].$$

Example 1 Assume that $(x, \sigma_{IV}) = (x_t, \sigma_{IVt})$ is a Gaussian sequence governed by the following special case of (5.1):

$$x_{t+1} = ax_t + b\epsilon_1(t+1), \quad \sigma_{IVt+1} = Ax_t + B\epsilon_2(t+1).$$

We will show that if $A \neq 0, b \neq 0, B \neq 0$, then the limiting error of filtering, $\gamma = \lim_{t \rightarrow \infty} \gamma_t$, exists. With the use of equation (5.1), we can get an expression for y_{t+1} :

$$\gamma_{t+1} = a^2 \gamma_t + \frac{a^2 A^2 \gamma_t^2}{B^2 + A^2 \gamma_t}.$$

If we let t tend to the infinity, we obtain

$$\gamma - a^2 \gamma - \frac{a^2 A^2 \gamma}{B^2 + A^2 \gamma} = 0.$$

After simplification of the equation, we get

$$\gamma^2 + \left[\frac{B^2 (1 - a^2)}{A^2} - b^2 \right] \gamma - \frac{b^2 B^2}{A^2} = 0. \quad (5.5)$$

We showed that the error of filtering is converging, and the limit is determined as the positive root of the equation (5.5).

The simple dynamic volatility skew is model in a state-space form (Harvey 1989). This time series of volatility skew estimation provide both cross-sectional information on the changes of the implied volatility across various strikes and temporal information on the time evolution of implied volatility. The measurement equation, according to (5.1), is given by:

$$\sigma_{K,t} = G_t x_t + D_t v_t, \quad (5.6)$$

where $\sigma_{K,t}$ is the general market implied volatility with the strike price K and the observed time t , G_t is the $t \times$ size(coefficients) matrix of strike/moneyness, x_t is the coefficient matrix. $D_t D_t' = \sigma_\epsilon^2 I$ represents the measurement noise covariance matrix, and $v_t \sim t(0, 1)$ are serially uncorrelated noise terms, independent of x_t . There were several studies on the parametric volatility curve fitting for the observed implied volatility. Mascia and Stewart [1], suggested a procedures of simple cubic polynomial interpolation against moneyness with Kalman Filter. According to Cont (2002), the implied volatility curve fitted against the function of the moneyness m has less deviation as compared to as a function of the strike K .

5.2 The cubic polynomial interpolation model

The approximation of the implied volatility by the cubic polynomial model has the following structure

$$\sigma_{pol} = x(1) + mx(2) + m^2x(3) + m^3x(4), \quad (5.7)$$

where σ_{pol} is the $t \times 1$ vector approximation of the implied volatility which fit against the function of moneyness m . (refer to section (3.1.2))

$x(1)$ estimates the level of the ATM implied volatility, $x(2)$, $x(3)$ and $x(4)$ capture the ATM slope, curvature and skewness, respectively.

The choice of cubic polynomial is easy to implement because it uses 4 coefficients to provide a fit to the observation volatility curves. We can further improve the accuracy of the curve fit using a higher order of polynomial interpolation. However, for using of the higher order polynomial, the growth of implied volatility introduces a negative density of the underlying asset when k increases. It was a fact mentioned in Christian Kahl which discussed by Roger Lee [10], Jim Gatheral [8].

5.3 The SVI model

In our study, we use Stochastic Volatility Inspired (SVI) ([4]). The SVI model of an estimation of the implied volatility has the following structure

$$\sigma_{SVI} = a + b \left(\rho(x - c) + \sqrt{(x - c)^2 + s^2} \right)$$

is a $t \times 1$ vector approximation of implied volatility which fit against the log forward moneyness x .

The Least Square estimation was introduced to measure the error between the observed Black-Scholes implied volatility and the SVI estimated implied volatility.

5.4 The Kalman filter estimation

The 3×1 state vector of the SVI parameters evolves under the system equation

$$x_t = a + Ux_{t-1} + Cu_t. \quad (5.8)$$

Multivariate autoregressive model was introduced to estimate the parameters of the a , U and C from (5.8).

- $a = A*\mu$, where A represents the 3×3 matrix consists of mean reversion coefficients on the main diagonal,
- μ is the vectors of the long run means,
- $U = I - A$,
- CC' is the covariance matrix of the error terms of the process,
- $u_t \sim N(0, 1)$ are uncorrelated disturbances and independent of X_{t-1} .

Finally, we denote $\hat{x}_t = \mathbb{E}_{t-1}[x_t]$ and $S_t = \text{Var}_{t-1}[x_t]$ before observing implied volatility $\sigma_{K,t}$. After that, we assume that initial distribution of x_1 is multivariate normal with known values for \hat{x}_1 and S_1 . According to Section (5.1), the optimal forecast \hat{x}_t for the skew coefficients x_t and the covariance S_t are related to the observed implied volatility $\sigma_{K,t}$. Then the new quantity evolves under the system equation is used to obtain the optimal forecast \hat{x}_{t+1} for the next state. By the Theorem (1) from Section (5.1) we get the following updating equations for expected value and covariance:

$$\begin{aligned} \hat{x}_{t+1} &= U [I - S_t G_t' T_t^{-1} G_t] \hat{x}_t + K_t \sigma_{K,t} + a, \\ S_{t+1} &= U [S_t - S_t G_t' T_t^{-1} G_t S_t] U' + CC', \end{aligned} \quad (5.9)$$

where $T_t = G_t S_t G_t' + \sigma_\epsilon^2 I$, and $K_t = U S_t G_t' T_t^{-1}$.

Chapter 6

Application of the Kalman filter to an option portfolio P&L forecasting

From the risk management perspective, the Kalman filter model can be implemented to forecast the risk potential of portfolios. The risk potential on the option portfolios can be detected as the sensitivity changes in the level, slope and curvatures of the implied volatility. This potential risk will then be translated into the P&L of the option portfolio.

6.1 The P-C-Parity

In financial mathematics, the Put-Call parity defines the relationship in an option portfolio of a call and a put with the same strike price and maturity time under no arbitrage condition

$$C - S = P - Ke^{-r(T-t)}. \quad (6.1)$$

6.2 The Portfolio 1: a Short Straddle

As mentioned in the section (3.2.1), we construct the short straddle portfolio which consists of short call and short put for ATM options. As the option portfolio consists of 2 ATM options, it is used to test a sensitivity to the changes in the level of the ATM implied volatility.

Using the P-C-parity (6.1), we reformulate the payout of the short straddle portfolio

$$V^{SS} = -C - P = -P + Ke^{-r(T-t)} - S - P = -2P - S + Ke^{-r(T-t)} \quad (6.2)$$

$$P = -\frac{1}{2} (V^{SS} - Ke^{-r(T-t)} + S) \quad (6.3)$$

At the money, $S = K$, the payoff of the put option is

$$P = Ke^{-r(T-t)} N(-d_2) - SN(-d_1). \quad (6.4)$$

Hence,

$$e^{-r(T-t)} N(-d_2) - N(-d_1) = \frac{1}{2} \left(\frac{V^{SS}}{S} - e^{-r(T-t)} + 1 \right), \quad (6.5)$$

where

$$\begin{aligned} d_1 &= \frac{(r - \frac{1}{2}\sigma^2)(T-t)}{\sigma\sqrt{T-t}} = \frac{(r + \frac{1}{2}\sigma^2)\sqrt{T-t}}{\sigma}, \\ d_2 &= d_1 - \sigma\sqrt{T-t}. \end{aligned} \quad (6.6)$$

6.3 The Portfolio 2: a Risk Reversal portfolio

To simulate a synthetic long underlying, the option portfolio can be formed as a short OTM put and a long OTM call. OTM put (K_-) and call (K_+) are equidistant from ATM level. The delta of the option measures the sensitivity of option prices relatives to the change of the underlying asset. For the long call option, the delta is always positive between 0 and 1. On the other hand, the put delta is in range from -1 to 0. We set the delta of the put at -0.25 delta and call at 0.25 . Then we formulate the payout for the long risk reversal portfolio as follow,

$$V^{RR} = C(K_+, \sigma_{SVI}(K_+, T)) - P(K_-, \sigma_{SVI}(K_-, T)). \quad (6.7)$$

The long risk-reversal portfolio is sensitive to the changes in the slope of the volatility curve that helps to measure the delta changes in the option portfolio.

6.4 Testing procedures of option portfolios

We proceed to assess the application function of the SVI Kalman filter model. Using the 1-day ahead forecast for the implied volatility by the SVI Kalman filter model, we input the forecasted implied volatility into the two option portfolios as mentioned above. We want to track the potential changes of the P&L valuation for the option portfolio over the defined period.

We proceed to assess the application function of the SVI Kalman Filter model. Using the 1-day aheas daily forecast function of the model, we track the changes in value of the option portfolios, over an observe period.

We introduced GARCH(1,1) model to forecast the underlying asset value S_{t+1} . As our main objective of the study is not focus on the forecasting of the underlying asset, therefore we suggest a simple and easy to use model to forecast the underlying asset value for time $t + 1$ at time $t = 0$.

From the forecasted value, we can derive the maximum and minimum of the forecasted underlying asset values between $S_{t+1}max$ and $S_{t+1}min$ interval of 95% confident level due to data set constraint. We used the forecasted underlying asset value to calculate the log forward moneyness matrix. This log forward moneyness matrix is used to generate the forecast coefficient vector for the implied volatility using the SVI kalman filter model at time $t = 0$. The forecasted implied volatility for time $t + 1$ is an input into the Black-Scholes model to generate the forecast for the option pricing for call and put option.

First of all, the option portfolios V^{xx} is constructed with the respective parameters $(S_t, K, r, T, t, \sigma)$ at time $t = 0$. We proceed to forecast the value of the option portfolios with the known fixed parameters (K, r, T, t) . Then we forecast underlying asset value S_{t+1} using GARCH(1,1) and the implied volatility using the SVI Kalman filte, which are an input is input into the Black-Scholes formula to derive the forecasted call and put option prices for the option portfolios.

The forecasted value of the option portfolio are compared to the initial value of the option portfolio at time $t = 0$ and the actual value of the option portfolios at time $t = 1$. Besides using this Kalman Filter model to measure the P&L value of the option portfolios, we further implemented a feature which helps to track the risk potential of the option portfolios.

The new feature introduced is useful to track the risk potential of option portfolios from the risk management perspective. Risk manager can easily track the risk of individual portfolios with the features.

We set a 95.45% confident interval range for the $S_{t+1}Max$ and $S_{t+1}Min$ for the movement of the underlying asset value, and the corresponding changes of the P&L value of the portfolios are refer to the delta changes for the option

portfolios which determine the risk potential of the option portfolios.

These procedures mentioned above can be implemented on various customization of the option portfolios, e.g. the Long Butterfly Spread which measures the sensitivity to the curvature of the volatility curve.

Chapter 7

Results

7.1 The Implied Volatility Result Analysis

In our previous chapters, we have suggested two models to generate the implied volatility. For a performance analysis, we require a better performance model to produce a higher accuracy of the forecasted implied volatility. The two suggested models have their respective strengths and weaknesses. We would like to conduct the performance analysis to compare their performance and accuracy for the implied volatility generated by the Black-Scholes implied volatility.

Although the increase of the order of the polynomial model can provide us with better accuracy of the curve fitting but the growth of the polynomial order leads to a negative density of the underlying asset, when the strike K increases. The higher order polynomial model opposed the fundamental restriction of the implied volatility curve parametrization which induces a non-negative density for the underlying assets. This fact has been analyzed and discussed in detail by Lee and Gatheral [10]. In order to tackle this issue and to achieve accurate curve fits, we introduce the SVI Kalman filter model.

Statistical data show that the SVI model has lower error rate as compared to the cubic polynomial model. Using the Least Square Estimation of errors, the SVI model generated an average error rate of 1.4731×10^{-6} and maximum error rate of 6.6460×10^{-6} . As compared to the cubic polynomial model generated an average error rate of 1.9190×10^{-6} and maximum error rate of 1.0750×10^{-5} . The model performance has improved by 23%. The figure (7.1) shows the LSE error measurement of the approximate implied volatility using the SVI model and the cubic polynomial model.

To observe the market volatility smile, we generate the implied volatility using the forecasted coefficient vectors for both the SVI model and the cubic

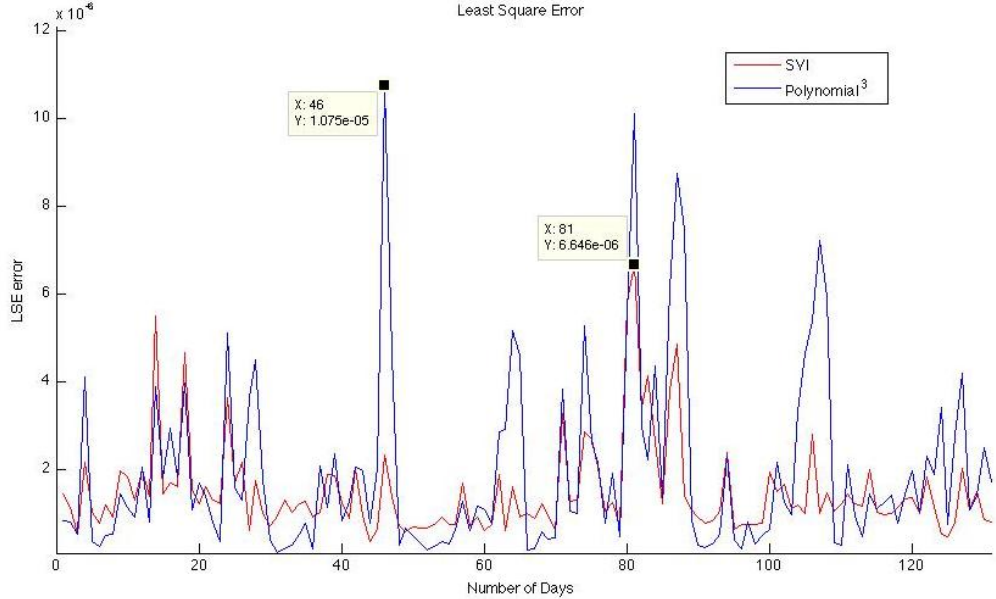


Figure 7.1. The LSE errors of the approximate implied volatility using the SVI and the cubic polynomial models.

polynomial model using the Kalman filter. The performance measurement shows that the SVI Kalman filter model has a higher accuracy and produced a lower LSE error rate as compared to the cubic polynomial Kalman filter model.

The figure (7.2) shows the LSE measurement of the approximated implied volatility using the SVI Kalman filter and the cubic polynomial Kalman filter models. The SVI Kalman filter model has the average error rate of 1.2484×10^{-6} and the maximum error rate of 8.0630×10^{-5} while the cubic polynomial Kalman filter model has the average error rate of 1.9362×10^{-6} and the maximum error rate of 3.8540×10^{-4} . The average error rate of the SVI Kalman filter has improved while the maximum error rate has significantly increased.

The figure shows the LSE measurement of the 1-day ahead forecasted implied volatility using the SVI Kalman filter model. From our performance results, we can observe that the SVI Kalman filter has a better forecast quality and we can use it to produce reliable 1-day ahead forecast of the implied volatility. The maximum error rate of the 1-day ahead forecast is 6.8020×10^{-5} .

In order to present the better accuracy performance of the SVI Kalman filter model, we have graphically displayed the 1-day ahead forecast of the SVI

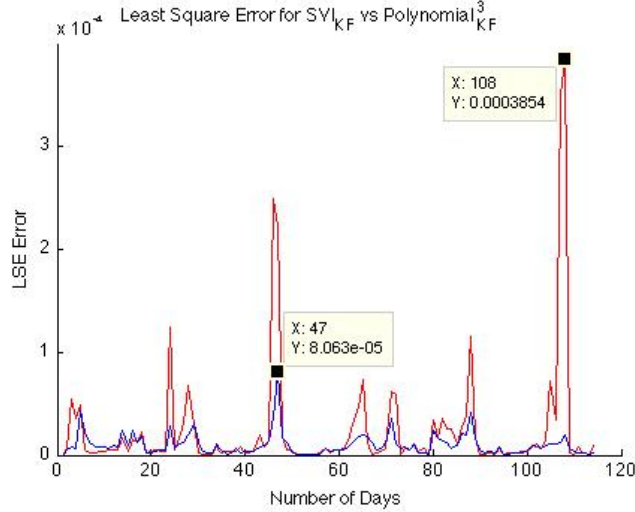


Figure 7.2. The LSE errors of the approximated implied volatility using the SVI Kalman filter and the cubic polynomial Kalman filter models.

Kalman filter implied volatility smile curve compare with the Black-Scholes implied volatility smile curve. The figure (7.4) shows both the minimum and maximum of the LSE error rate for the 1-day ahead forecast of the SVI Kalman filter model, the minimum LSE error rate is equal to 2.5526×10^{-6} and the maximum error rate is equal to 6.8020×10^{-5} .

7.2 The Portfolios Result Analysis

As mentioned in Chapter 6, we have introduced the use of the SVI Kalman filter for the option portfolio's profit and loss (P&L) forecasting. This Kalman filter extrapolating techniques is implemented on the following two index option portfolios, i.e the Short Straddle and the Long Risk Reversal.

7.2.1 The Portfolio of a Short Straddle (V^{SS})

As mentioned in Chapter 6.4, we followed the step by step testing procedures for the forecasting of the implied volatility using the SVI Kalman filter model.

The plot (??) shows the minimum and the maximum changes for the portfolio of a Short Straddle. The red cross marks the initial P&L value of the option portfolio at time $t = 0$. The black solid line displays the forecasting value of the option portfolio with respect to the changes of the forecasting

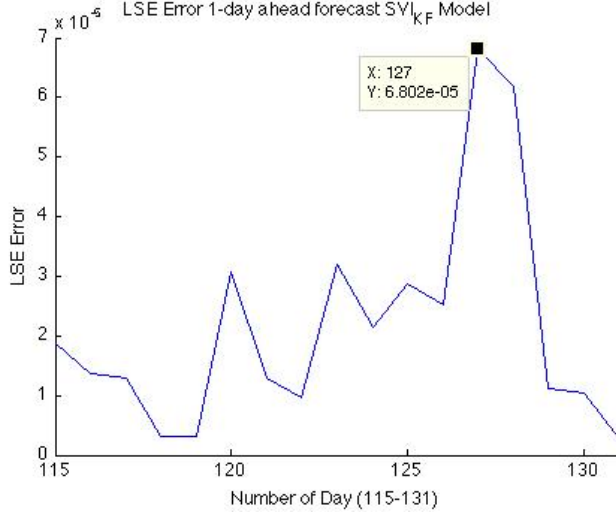


Figure 7.3. The LSE errors of the forecasted implied volatility using the SVI Kalman filter model.

underlying asset value S_{t+1} at time $t = 0$. The blue and red circles along the black line mark the minimum and maximum of the forecasting underlying asset value $S_{t+1}Min$ and $S_{t+1}Max$, respectively. The green cross marks the position for the forecasting P&L of the option portfolios at time $t = 0$ while the red cross shows the actual P&L of the option portfolios at time $t = 1$.

On the y -axis, it marks the delta changes which define the range of the forecasting value changes of option portfolio with respect to the interval between $S_{t+1}Min$ and $S_{t+1}Max$. The following figure displays the minimum and maximum delta changes for the option short straddle V^{SS} .

7.2.2 The Portfolio of the Long Risk Reversal (V^{RR})

The plot presents the minimum and the maximum changes of the values of the portfolio of the Long Risk Reversal. The red cross marks the initial P&L value of the option portfolio at time $t = 0$. The black solid line displays the forecasting value of the option portfolio with respect to the changes of the forecasting underlying asset value S_{t+1} at time $t = 0$. The blue and red circles along the black line mark the minimum and maximum of the forecasting underlying asset value $S_{t+1}Min$ and $S_{t+1}Max$, respectively. The green cross marks the position for the forecasting P&L of the option portfolios at time $t = 0$ while the red cross shows the actual P&L of the option portfolios at time $t = 1$.

On the y -axis, it marks the delta changes which define the range for the

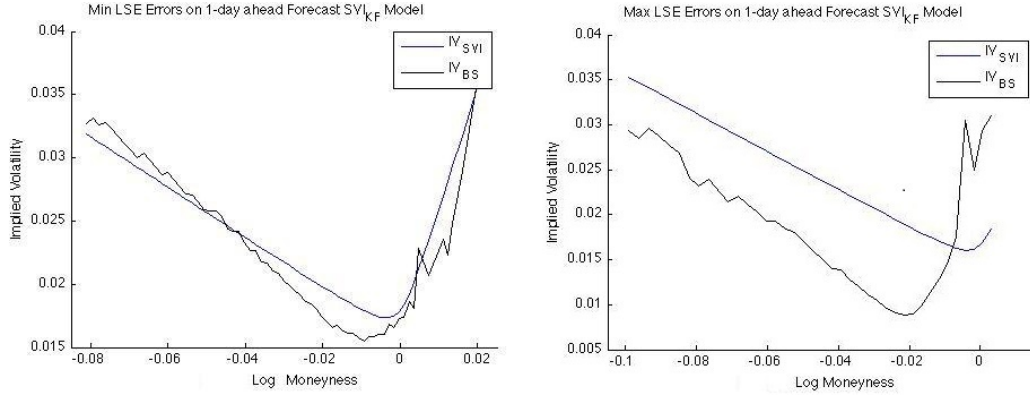


Figure 7.4. The minimum and maximum errors of the 1-day ahead forecasted implied volatility using the SVI Kalman filter model.

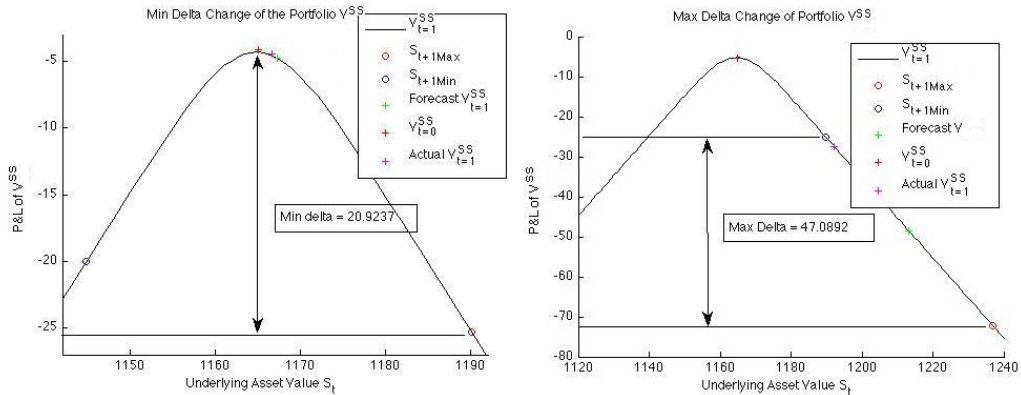


Figure 7.5. The minimum and maximum delta changes for the portfolio of a short straddle.

forecasted changes of the option portfolio value with respect to the interval between $S_{t+1}Min$ and $S_{t+1}Max$. The following figure displays the minimum and maximum delta changes of the forecasted option portfolio called the Long Risk Reversal V^{RR} .

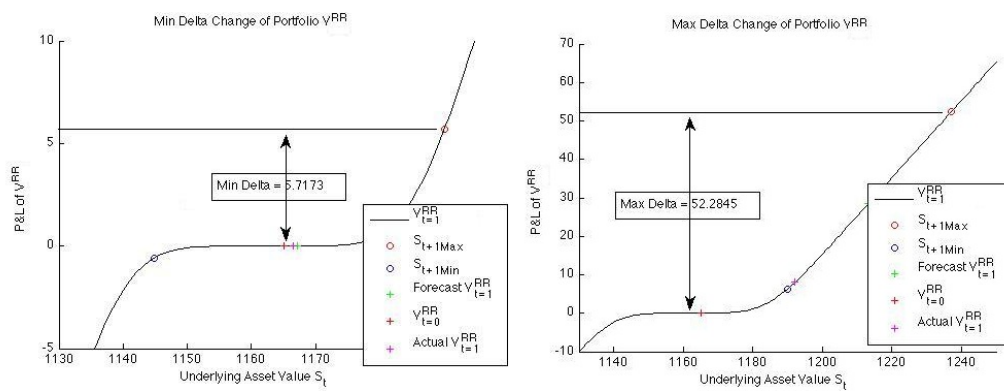


Figure 7.6. The minimum and maximum delta changes for the portfolio of the long risk reversal.

Chapter 8

Conclusions

The study presents the Kalman filter procedures for the SVI approximation model of the implied volatility. We have successfully replaced the existing cubic polynomial model with the suggested SVI model due to the better accuracy. The statistical data shows that the SVI model produced a more accurate forecasting result.

In addition, we have also implemented the application for the SVI Kalman filter model to forecast the P&L of the option portfolio such as Short straddle and Long risk reversal option. This Kalman filter extrapolating technique helps to produce 1-day ahead forecasting of the P&L of the option portfolios.

For the applications, such as risk management of the portfolio and the option pricing, we need to customize our existing SVI Kalman Filter to forecast the 1-day ahead implied volatility of an underlying asset and to predict the desirable range on the volatility changes. These are translated into the special features that we can track the delta changes of the P&L of the option portfolios for better managing of the potential risk of the portfolios.

Given the time constraint, we managed to meet all the objectives listed for the research and implemented some new features. This study can be more accurate with better database. This can further reduce the error with more accurate forecasting of the coefficient vectors of the implied volatility and the parameters of the Kalman filter model.

Finally, this model can be better calibrated and implemented with the study of the term structure volatility and the volatility surfaces of the implied volatility. This gives us macro understanding of the dynamic of the implied volatility.

Bibliography

- [1] Mascia Bedendo, Steward D. Hodges (2009)
The dynamics of the volatility skew: a Kalman filter approach. Journal of Banking & Finance, **33**, 1156 – 1165.
- [2] ALBERT N. SHIRYAEV (1996)
Probability. New York: Springer-Verlag.
- [3] ALBERT N. SHIRYAEV (1999)
Essentials of stochastic finance. Singapore: World Scientific.
- [4] JIM GATHERAL (2004)
The volatility surface: a practitioner's guide. Wiley Finance.
- [5] REINHOLD HAFNER (2004)
Stochastic implied volatility: a factor-based model. Berlin: Springer-Verlag.
- [6] PAUL WILMOTT (2006)
Paul Wilmott on quantitative finance. John Wiley & Sons, Inc.
- [7] SHELDON NARENBERG (1994)
Option volatility & pricing. USA: McGraw-Hill.
- [8] JIM GATHERAL (May, 2004)
A parsimonious arbitrage-free implied volatility parameterization with application to the volatility derivatives. Global Derivatives & Risk Management:
http://www.math.nyu.edu/fellows_fin_math/gatheral/madrid2004.pdf
- [9] LIFFE ADMINISTRATION AND MANAGEMENT (2002)
LIFFE options: a guide to trading strategies & pricing. LIFFE.
- [10] ROGER W. LEE (November 22, 2002)
Implied volatility: statics, dynamics and probabilistic interpretation. Recent advances in applied probability. Berlin: Springer Verlag.

- [11] B. DUPIRE (January, 1994)
Pricing with a smile. Risk, 18–20.
- [12] JOHN C. HULL (1997)
Options, futures and other derivative securities. Prentice Hall.
- [13] CHRISTIAN KAHL (2007)
Modelling and simulation of stochastic volatility in finance. Dissertation.Com, Florida.
- [14] ZELIADE SYSTEMS SAS (September, 2009)
Quasi-explicit calibration of Gatheral's SVI model.
<http://www.zeliade.com/whitepapers/zwp-0005.pdf>
- [15] SIMON HAYKIN (2001)
Kalman filtering and Neural Networks. John Wiley & Sons, Inc
- [16] GREG WELCH, GARY BISHOP (Updated 2006)
An Introduction to Kalman Filter. University of North Carolina at Chapel Hill: <http://www.cs.unc.edu/~welch/kalman/kalmanIntro.html>
- [17] CAROL ALEXANDER, LEONARDO M. NOGUEIRA (2008)
Stochastic Local Volatility. SSRN: <http://ssrn.com/abstract=1107685>
- [18] Peter Carr, Liuren Wu (October 2007)
Stochastic Skew for Currency Options. Journal of Financial Economics, 213 – 247.
- [19] JIM GATHERAL, ANTOINE JACQUIER (February 18, 2010)
Convergence of Heston to SVI.
SSRN: <http://ssrn.com/abstract=1555251>
- [20] ANDREW C. HARVEY, NEIL SHEPHARD (1993)
Structural Time Series Models, Handbook of Statistics, Vol 11. Elsevier Science Publishers B. V.
- [21] R. Cont, J. Da Fonseca (2002)
Dynamics of Implied Volatility Surfaces. Quantitative Finance, **2(1)**, 45 – 60
- [22] R. Cont, J. Da Fonseca, V. Durrleman (2002)
Stochastic Models of Implied Volatility Surfaces. Economic Notes, **no. 2-2002**, 361 – 377

- [23] Nabil Kahale (March 2005)
Smile Interpolation and Calibration of the Local Volatility Model. Risk Magazine.

Appendix

8.1 The Least Square Method

The method of the least squares is a standard approach to the approximate solution of overdetermined systems, i.e. sets of equations in which there are more equations than unknowns. “Least” squares means that the overall solution minimizes the sum of the squares of the errors made in solving every single equation. The most important application is in data fitting. The best fit in the least-squares sense minimizes the sum of squared residuals, a residual being the difference between an observed value and the fitted value provided by a model.

The objective consists of adjusting the parameters of a model function to best fit a data set. A simple data set consists of n points (data pairs) (x_i, y_i) , $i = 1, \dots, n$, where x_i is an independent variable and y_i is a dependent variable whose value is found by observation. The model function has the form $f(x, \beta)$, where the m adjustable parameters are held in the vector β . The goal is to find the parameter values for the model which “best” fits the data. The least squares method finds its optimum when the sum, S , of squared residuals

$$S = \sum_{i=1}^n r_i^2 \quad (8.1)$$

is a minimum. A residual is defined as the difference between the value predicted by the model and the actual value of the dependent variable

$$r_i = y_i - f(x_i, \beta). \quad (8.2)$$

The minimum of the sum of squares is found by setting the gradient to zero. Since the model contains m parameters there are m gradient equations.

$$\frac{\partial S}{\partial \beta_j} = 2 \sum_i r_i \frac{\partial r_i}{\partial \beta_j} = 0, \quad j = 1, \dots, m \quad (8.3)$$

and since $r_i = y_i - f(x_i, \beta)$ the gradient equations become

$$-2 \sum_i \frac{\partial f(x_i, \beta)}{\partial \beta_j} r_i = 0, \quad j = 1, \dots, m \quad (8.4)$$

The gradient equations apply to all least squares problems. Each particular problem requires particular expressions for the model and its partial derivatives.

A regression model is a linear one when the model comprises a linear combination of the parameters, i.e.

$$f(x_i, \beta) = \sum_{j=1}^m \beta_j \phi_j(x_i) \quad (8.5)$$

where the coefficients, ϕ_j , are functions of x_i . Letting

$$X_{ij} = \frac{\partial f(x_i, \beta)}{\partial \beta_j} = \phi_j(x_i), \quad (8.6)$$

we can then see that in that case the least square estimate (or estimator, in the context of a random sample), $\hat{\beta}$ is given by

$$\hat{\beta} = (X^T X)^{-1} X^T y. \quad (8.7)$$